

Real-Time Diagrammatic Theory of Electron Waiting Time Distributions: Interaction Effects and Higher-Order Tunneling Processes

Philipp Stegmann,¹ Björn Sothmann,¹ Jürgen König,¹ and Christian Flindt²

¹*Theoretische Physik, Universität Duisburg-Essen and CENIDE, 47048 Duisburg, Germany*

²*Department of Applied Physics, Aalto University, 00076 Aalto, Finland*

(Dated: May 25, 2022)

We develop a real-time diagrammatic theory of electron waiting time distributions for quantum transport in strongly interacting nanostructures. While existing methods address either weakly coupled systems with strong Coulomb interactions or coherent transport in mesoscopic conductors without interactions, our approach makes it possible to treat the interesting intermediate regime where both interaction effects and higher-order tunneling processes are important. As an illustration of experimental relevance, we consider a quantum dot coupled to electronic reservoirs and find that the distribution of waiting times between transferred electrons is drastically affected by virtual charge fluctuations and higher-order tunneling processes such as cotunneling that lead to non-Markovian dynamics on the quantum dot, and which can now be accounted for by our theoretical framework.

Introduction.— Electronic waiting time distributions are an important concept in the analysis of quantum transport in nano-scale structures [1–36]. Unlike full counting statistics, which typically considers the time-integrated current fluctuations [37, 38], waiting time distributions are concerned with the short time-span that passes between consecutive charge transfers in a nano-scale conductor. The waiting time distribution contains a wealth of information about the underlying transport processes. For example, it has been predicted that the waiting time distribution for a quantum point contact should exhibit a cross-over from Wigner-Dyson statistics at full transmission to Poisson statistics close to pinch-off [4, 9], illustrating a profound connection between free fermions and the eigenvalues of large matrices [39].

Among many interesting applications, waiting time distributions have been used to characterize dynamic single-electron emitters [3, 7, 19, 22] and to identify Andreev processes and Majorana states at superconductor-normal-metal interfaces [5, 15, 16, 26, 36]. In addition to this theoretical progress, waiting time distributions have been measured in several recent experiments [40–43]. On the theory side, electron waiting time distributions have been considered in two opposite limits. For sequential tunneling in Coulomb-blockade structures, the waiting time distribution can be obtained from a master-equation description of charge transport [1, 3, 35]. In the other regime of phase-coherent transport of non-interacting electrons, the waiting time distribution can be evaluated using scattering theory [4, 7, 9], tight-binding calculations [12], or Green’s function methods [11, 14]. However, for the interesting intermediate regime where both interaction effects and higher-order tunneling processes are important, a systematic theory of electronic waiting time distributions has so far been lacking.

In this Letter, we develop a real-time diagrammatic theory of electron waiting time distributions for quantum transport in strongly interacting nanostructures. By combining non-Markovian master equations [6] with

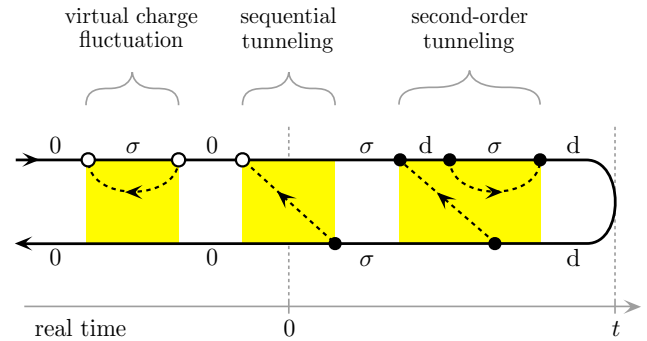


FIG. 1. Real-time dynamics on the Keldysh contour. Wick contractions of reservoir operators are shown as dashed lines. Counted tunneling vertices after $t = 0$ are shown as filled circles, while earlier ones are indicated by open circles.

the real-time diagrammatic approach to quantum transport [44–46], we devise a systematic method to include higher-order tunneling processes such as co-tunneling and pair tunneling in the distribution of electron waiting times. Co-tunneling processes can be described at the level of mean currents using T -matrix approaches [45–47], which, however, cannot account for non-Markovian effects that influence the charge transport fluctuations beyond average values [48, 49]. Motivated by the recent experiments on waiting time distributions [40–43], we consider tunneling between a quantum dot and external reservoirs and find that the waiting time distribution is strongly influenced by virtual charge fluctuations that are included in the real-time diagrams shown in Fig. 1.

Generalized master equation.— We consider charge tunneling in a nano-scale system whose dynamics is governed by the non-Markovian master equation [48–50]

$$\frac{d}{dt}\hat{\rho}_N(t) = \sum_{N'} \int_0^t dt' \mathbb{W}_{N-N'}(t-t')\hat{\rho}_{N'}(t') + \hat{\gamma}_N(t). \quad (1)$$

Here, the reduced density matrix of the system $\hat{\rho}_N(t)$ is

obtained by tracing out the degrees of freedom associated with the external reservoirs. Moreover, the density matrix is resolved with respect to the number of transferred particles, so that $P_N(t) = \text{Tr}[\hat{\rho}_N(t)]$ is the probability that $N \geq 0$ electrons have tunneled into the reservoirs during the time span $[0, t]$ [38]. Non-Markovian master equations of this form naturally arise in the real-time diagrammatic approach to quantum transport [44–46] or in the Nakajima-Zwanzig projection method for open quantum systems [51]. The kernel \mathbb{W} describes the non-Markovian time evolution of the system and depends only on the time difference $t - t'$ in the absence of time-dependent perturbations. In addition, the inhomogeneity

$$\hat{\gamma}_N(t) = \sum_{N'} \int_{-\infty}^0 dt' \widetilde{\mathbb{W}}_{N-N'}(t, t') \hat{\rho}_{\text{stat}} \quad (2)$$

is crucial for a proper inclusion of correlations that build up between the system and its environment before the counting of particles begins at $t = 0$ [6, 49–53]. These correlations decay with time and do not influence the low-frequency fluctuations of the charge transport. On the other hand, they are important at short times, which is relevant in the context of waiting time distributions. The inhomogeneity is expressed in terms of the modified kernel $\widetilde{\mathbb{W}}$, which (in contrast to \mathbb{W}) extends to times before $t = 0$, when the counting of electrons begins. Technically, the modified kernel includes tunneling vertices that are not counted as indicated by open circles on the Keldysh contour in Fig. 1 [52, 53]. Moreover, it depends both on t and t' and not only on their difference, since the beginning of charge counting at $t = 0$ breaks the translation invariance in time. The system itself evolves from an arbitrary state in the far past and is assumed to have reached its stationary state $\hat{\rho}_{\text{stat}}$ well before $t = 0$.

Solving the generalized master equation is a formidable

task. However, we can use an operator-valued generalization of the standard generating function technique in Laplace space by introducing the transformed density matrix $\hat{\rho}_s(z) = \int_0^\infty dt e^{-zt} \sum_N s^N \hat{\rho}_N(t)$ together with similar definitions for the kernel and the inhomogeneity. Setting $s = 1$ traces out the number of transferred particles and yields the stationary state from $\mathbb{W}_{s=1}(z = 0) \hat{\rho}_{\text{stat}} = 0$ with the normalization $\text{Tr}\{\hat{\rho}_{\text{stat}}\} = 1$. Using these definitions, the solution of Eq. (1) becomes [6, 49]

$$\hat{\rho}_s(z) = \frac{1}{z - \mathbb{W}_s(z)} [\hat{\rho}_{\text{stat}} + \hat{\gamma}_s(z)], \quad (3)$$

which is a powerful formal result that in principle yields the full distribution of transferred charge for any observation time. As we now will show, it also leads to a systematic theory of electron waiting times in nano-scale conductors, which can include both interaction effects and higher-order tunneling processes.

Electron waiting times.— The waiting time distribution is the probability density that two consecutive tunneling events are separated by the time τ [1]. In recent years, waiting time distributions have been investigated theoretically for quantum transport in mesoscopic conductors and for weakly coupled Coulomb-blockade devices [1–36]. In addition, several experiments have measured waiting time distributions in nano-structures using charge detectors [40–42]. For stationary processes, the waiting time distribution can be expressed as $w(\tau) = \langle \tau \rangle \partial_\tau^2 \Pi(\tau)$, where $\langle \tau \rangle = -1/[\partial_\tau \Pi(0)]$ is the mean waiting time, and $\Pi(\tau) = P_{N=0}(\tau)$ is the idle-time probability that no transfers have occurred during the time span $[0, \tau]$ [4, 9]. Importantly, the idle-time probability can be obtained from Eq. (3) using that $\Pi(z) = \text{Tr}\{\hat{\rho}_{s=0}(z)\}$. Expanding the kernel around $z = 0$, we can then return to the time domain and arrive at the expression

$$w(\tau) = \langle \tau \rangle \sum_{m,k=0}^{\infty} \frac{1}{m! k!} \text{Tr} \left\{ \partial_z^m \left[\mathcal{J}(z) \mathbb{W}_0^{m+k}(z) e^{\mathbb{W}_0(z)\tau} \right] \partial_z^k \left[\mathcal{J}(z) + \tilde{\mathcal{J}}(z) \right] \hat{\rho}_{\text{stat}} \right\}_{z=0}, \quad (4)$$

which is completely general and enables a systematic, perturbative analysis of how tunneling processes of different orders, indicated by yellow diagrams in Fig. 1, contribute to the distribution of waiting times. Here, we have defined the jump operators $\mathcal{J}(z) = \mathbb{W}_1(z) - \mathbb{W}_0(z)$ and $\tilde{\mathcal{J}}(z) = \int_0^\infty dt z e^{-zt} \int_{-\infty}^0 dt' [\widetilde{\mathbb{W}}_1(t, t') - \widetilde{\mathbb{W}}_0(t, t')]$, and we note that memory effects are encoded in non-zero derivatives with respect to z . Thus, only the lowest order term ($k, m = 0$) remains in the Markovian limit, where we recover the well-known result [1]

$$w^{\text{M}}(\tau) = \langle \tau \rangle^{\text{M}} \text{Tr} \left[\mathcal{J} e^{\mathbb{W}_0 \tau} \mathcal{J} \hat{\rho}_{\text{stat}} \right], \quad (5)$$

since the kernel and the jump operators in that case do not depend on z and the inhomogeneity vanishes.

Quantum dot.— We are now ready to apply our general theoretical framework to a physical system of experimental relevance. We first consider a quantum dot coupled to a single electrode. The full Hamiltonian reads $\hat{\mathcal{H}} = \hat{\mathcal{H}}_{\text{res}} + \hat{\mathcal{H}}_{\text{qs}} + \hat{\mathcal{H}}_{\text{tun}}$, where $\hat{\mathcal{H}}_{\text{res}} = \sum_{\mathbf{k}\sigma} \varepsilon_{\mathbf{k}\sigma} \hat{a}_{\mathbf{k}\sigma}^\dagger \hat{a}_{\mathbf{k}\sigma}$ describes the reservoir of non-interacting electrons. The quantum dot, $\hat{\mathcal{H}}_{\text{qs}} = \sum_{\sigma} \varepsilon_{\sigma} \hat{d}_{\sigma}^\dagger \hat{d}_{\sigma} + U \hat{d}_{\uparrow}^\dagger \hat{d}_{\uparrow} \hat{d}_{\downarrow}^\dagger \hat{d}_{\downarrow}$, can be either empty $|0\rangle$, occupied by a single electron $|\sigma\rangle$ with spin $\sigma = \uparrow, \downarrow$, or doubly occupied $|d\rangle$, with U denoting the Coulomb interactions on the quantum dot. An applied

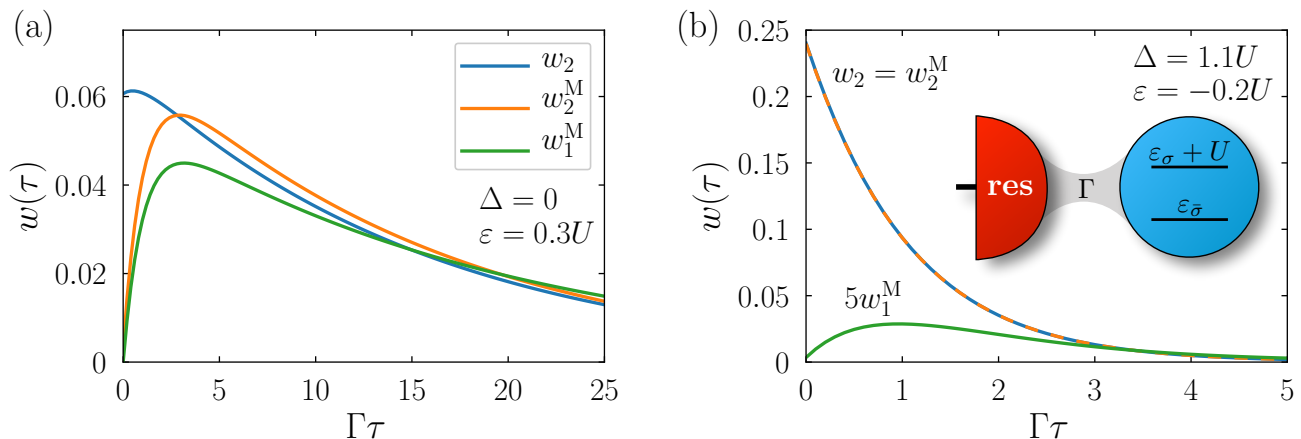


FIG. 2. Distribution of electron waiting times. The non-Markovian expression (4) is evaluated up to second order in the tunnel coupling Γ (blue curve), while the Markovian approximation (5) is evaluated up to first (green) and second order (orange). The parameters are $k_B T = U/12$ and $\hbar\Gamma = U/60$, with the left and right panels corresponding to different gatings of the quantum dot. The system is sketched in the inset of (b), showing the relevant excitation energies of the quantum dot.

magnetic field lifts the degeneracy of spin-up, $\varepsilon_\uparrow = \varepsilon + \frac{\Delta}{2}$, and spin-down electrons, $\varepsilon_\downarrow = \varepsilon - \frac{\Delta}{2}$, where Δ is the Zeeman splitting. The orbital energy ε relative to the Fermi level of the reservoir can be tuned by an external gate voltage. Electron tunneling between the quantum dot and the reservoir is governed by the Hamiltonian $\hat{\mathcal{H}}_{\text{tun}} = \sum_{\mathbf{k}\sigma} (g \hat{a}_{\mathbf{k}\sigma}^\dagger \hat{d}_\sigma + g^* \hat{d}_\sigma^\dagger \hat{a}_{\mathbf{k}\sigma})$, and the tunnel coupling is related to the tunnel matrix elements as $\Gamma = 2\pi|g|^2\nu$, where ν is the density of states in the lead.

To evaluate the waiting times between electrons tunneling into the reservoir, we expand the kernel order-by-order in the tunneling coupling Γ as $\mathbb{W}_s(z) = \sum_{i=1}^{\infty} \mathbb{W}_s^{(i)}(z)$, with similar expressions for the jump operators and the density matrix. Each term is evaluated using the real-time diagrammatic technique for quantum transport in nano-structures [44–46]. For each diagram in Fig. 1, we count the number of black tunneling vertices involving a factor of g on the upper Keldysh contour or a factor of g^* on the lower contour, minus the number of black tunneling vertices involving a factor of g^* on the upper contour or a factor of g on the lower contour [54]. Within this framework, we evaluate the expression for the waiting time distribution in Eq. (4) up to second order in the coupling, $w_2(\tau)$, and the Markovian approximation (5) to first, $w_1^M(\tau)$, and second order, $w_2^M(\tau)$.

Waiting time distributions.— Figure 2 shows waiting time distributions obtained with our non-Markovian theory and the Markovian approximation. The Markovian approximations both show a strong suppression at short times. Within these approximations, two electrons are unlikely to leave the quantum dot almost simultaneously because of the strong Coulomb interactions, which prevent the quantum dot from being doubly occupied. After a finite time span, the quantum dot can be re-filled, and the suppression is lifted before the distribu-

tions eventually vanish at long times. By contrast, our non-Markovian theory reveals a different physical picture with the suppression at short times lifted by the higher-order processes that are now fully included. Specifically, the systematic evaluation of the kernel involves physical mechanisms like virtual charge fluctuations between the quantum dot and the reservoir given by the left diagram in Fig. 1. The right diagram corresponds to a second-order tunneling process that includes a virtual charge fluctuation, giving rise to a Lamb shift of the energy splitting between initial and final states. These processes are already included to second order within the Markovian approximation. However, to fully account for the induced memory effects, our non-Markovian framework is needed. The memory effects are clearly important for the waiting time distributions in Fig. 2(a), where the quantum dot level is situated well above the Fermi level of the reservoir, and the quantum dot is mostly empty. By contrast, in Fig. 2(b), where we have shifted the quantum dot level below the Fermi level, the memory effects become negligible, even if a proper inclusion of the higher-order processes remains crucial for the Markovian approximations. In particular, if only first-order processes are included, important short-time processes are missed, and the typical waiting times are substantially overestimated.

Transport setup.— In Fig. 3, we go on to consider a transport setup, where a bias-voltage between two electrodes drives a current through the quantum dot. We evaluate the waiting time distribution between electrons tunneling into the drain electrode based on Eq. (4) up to second order in the equal couplings to the source and the drain electrodes, $\Gamma_S = \Gamma_D$. Figure 3(a) shows a conductance map as a function of the bias-voltage V and the gate voltage, which controls the energy level ε of the quantum dot. In the low-bias regime, Coulomb block-

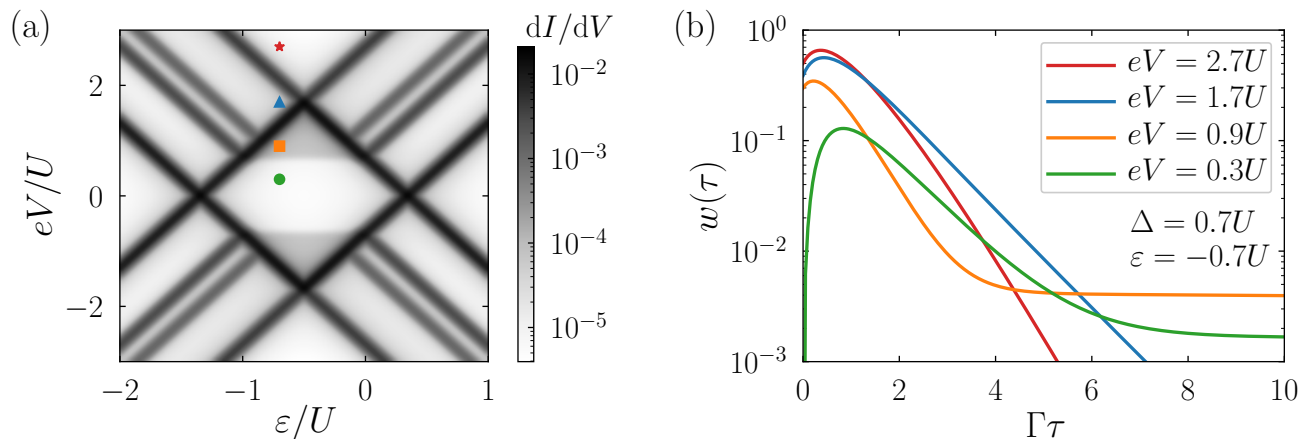


FIG. 3. Waiting time distributions for a transport setup. A bias between two electrodes drives a current through the quantum dot. (a) Differential conductance as a function of the bias-voltage and the gate-voltage. Parameters are $k_B T = U/60$, $\Delta = 0.7U$, and $\hbar\Gamma_S = \hbar\Gamma_D \equiv \hbar\Gamma = U/300$. (b) Waiting time distributions corresponding to the four points in the conductance map.

ade suppresses the current through the quantum dot, and elastic cotunneling is the dominant transport mechanism. With an increasing voltage, additional transport processes are activated; first inelastic cotunneling, then sequential tunneling, and eventually all excitations are inside the bias window such that the strong Coulomb interactions effectively become irrelevant.

Figure 3(b) shows waiting time distributions corresponding to the four points in the conductance map. At low voltages, the waiting time distribution is suppressed at short times, showing that elastic cotunneling processes very rarely occur simultaneously. While the distribution for short times is affected by the non-Markovian dynamics, the tail can be captured by a Markovian approximation, similar to what was used in a recent work on cotunneling [30]. As the voltage is increased, the suppression at short times is lifted because of inelastic cotunneling which now becomes possible. Moreover, the distribution becomes biexponential with the long tail determined by the slow second-order process depicted in the right diagram of Fig. 1 that occurs in addition to elastic cotunneling. As the voltage is further increased, sequential tunneling becomes the main transport mechanism, and the tail gradually vanishes. Still, the distribution is not suppressed at short times due to the higher-order processes that occur together with sequential tunneling.

Conclusions.— We have developed a real-time diagrammatic theory of electron waiting time distributions that enables a systematic description of interaction effects and higher-order tunneling processes. Our theoretical framework bridges the gap between non-interacting theories of electron waiting times, valid for phase-coherent transport in mesoscopic conductors, and master-equation descriptions, which apply to sequential tunneling in nano-structures with strong interactions. As an illustrative application, we have considered the charge

fluctuations between a quantum system, such as a quantum dot, an impurity, or a molecule, and external reservoirs. We have shown that the waiting time distributions are strongly affected by higher-order tunneling processes including virtual charge fluctuations between the quantum dot and the electrode, which give rise to non-Markovian dynamics. Our work paves the way for future investigations of waiting time distributions in systems with strong correlations, for example close to a Kondo resonance [55, 56] or in a Luttinger liquid [57, 58].

Acknowledgements.— We thank A. Braggio for useful discussions. This work was supported by the German Research Foundation (DFG) within the Collaborative Research Centre (SFB) 1242 “Non-Equilibrium Dynamics of Condensed Matter in the Time Domain” (Project No. 278162697) and the Ministry of Innovation NRW via the “Programm zur Förderung der Rückkehr des Hochqualifizierten Forschungsnachwuchses aus dem Ausland”. The work of CF was supported by the Academy of Finland (Projects No. 308515 and No. 312299). PS acknowledges support from the German National Academy of Sciences Leopoldina (Grant No. LPDS 2019-10).

-
- [1] T. Brandes, Waiting times and noise in single particle transport, *Ann. Phys.* **17**, 477 (2008).
 - [2] S. Welack, S. Mukamel, and Y. Yan, Waiting time distributions of electron transfers through quantum dot Aharonov-Bohm interferometers, *Europhys. Lett.* **85**, 57008 (2009).
 - [3] M. Albert, C. Flindt, and M. Büttiker, Distributions of Waiting Times of Dynamic Single-Electron Emitters, *Phys. Rev. Lett.* **107**, 086805 (2011).
 - [4] M. Albert, G. Haack, C. Flindt, and M. Büttiker, Electron Waiting Times in Mesoscopic Conductors, *Phys. Rev. Lett.* **108**, 186806 (2012).

- [5] L. Rajabi, C. Pörtl, and M. Governale, Waiting Time Distributions for the Transport through a Quantum-Dot Tunnel Coupled to One Normal and One Superconducting Lead, *Phys. Rev. Lett.* **111**, 067002 (2013).
- [6] K. H. Thomas and C. Flindt, Electron waiting times in non-Markovian quantum transport, *Phys. Rev. B* **87**, 121405 (2013).
- [7] D. Dasenbrook, C. Flindt, and M. Büttiker, Floquet Theory of Electron Waiting Times in Quantum-Coherent Conductors, *Phys. Rev. Lett.* **112**, 146801 (2014).
- [8] M. Albert and P. Devillard, Waiting time distribution for trains of quantized electron pulses, *Phys. Rev. B* **90**, 035431 (2014).
- [9] G. Haack, M. Albert, and C. Flindt, Distributions of electron waiting times in quantum-coherent conductors, *Phys. Rev. B* **90**, 205429 (2014).
- [10] B. Sothmann, Electronic waiting-time distribution of a quantum-dot spin valve, *Phys. Rev. B* **90**, 155315 (2014).
- [11] G.-M. Tang, F. Xu, and J. Wang, Waiting time distribution of quantum electronic transport in the transient regime, *Phys. Rev. B* **89**, 205310 (2014).
- [12] K. H. Thomas and C. Flindt, Waiting time distributions of noninteracting fermions on a tight-binding chain, *Phys. Rev. B* **89**, 245420 (2014).
- [13] D. Dasenbrook, P. P. Hofer, and C. Flindt, Electron waiting times in coherent conductors are correlated, *Phys. Rev. B* **91**, 195420 (2015).
- [14] R. Seoane Souto, R. Avriller, R. C. Monreal, A. Martín-Rodero, and A. Levy Yeyati, Transient dynamics and waiting time distribution of molecular junctions in the polaronic regime, *Phys. Rev. B* **92**, 125435 (2015).
- [15] D. Chevallier, M. Albert, and P. Devillard, Probing Majorana and Andreev bound states with waiting times, *Europhys. Lett.* **116**, 27005 (2016).
- [16] M. Albert, D. Chevallier, and P. Devillard, Waiting times of entangled electrons in normal-superconducting junctions, *Physica E* **76**, 209 (2016).
- [17] T. Brandes and C. Emary, Feedback control of waiting times, *Phys. Rev. E* **93**, 042103 (2016).
- [18] D. Dasenbrook and C. Flindt, Quantum theory of an electron waiting time clock, *Phys. Rev. B* **93**, 245409 (2016).
- [19] P. P. Hofer, D. Dasenbrook, and C. Flindt, Electron waiting times for the mesoscopic capacitor, *Physica E* **82**, 3 (2016).
- [20] S. L. Rudge and D. S. Kosov, Distribution of residence times as a marker to distinguish different pathways for quantum transport, *Phys. Rev. E* **94**, 042134 (2016).
- [21] D. S. Kosov, Waiting time distribution for electron transport in a molecular junction with electron-vibration interaction, *J. Chem. Phys.* **146**, 074102 (2017).
- [22] E. Potanina and C. Flindt, Electron waiting times of a periodically driven single-electron turnstile, *Phys. Rev. B* **96**, 045420 (2017).
- [23] K. Ptasiński, Waiting time distribution revealing the internal spin dynamics in a double quantum dot, *Phys. Rev. B* **96**, 035409 (2017).
- [24] K. Ptasiński, Nonrenewal statistics in transport through quantum dots, *Phys. Rev. B* **95**, 045306 (2017).
- [25] K. Ptasiński, First-passage times in renewal and nonrenewal systems, *Phys. Rev. E* **97**, 012127 (2018).
- [26] N. Walldorf, C. Padurariu, A.-P. Jauho, and C. Flindt, Electron Waiting Times of a Cooper Pair Splitter, *Phys. Rev. Lett.* **120**, 087701 (2018).
- [27] G. Tang, F. Xu, S. Mi, and J. Wang, Spin-resolved electron waiting times in a quantum-dot spin valve, *Phys. Rev. B* **97**, 165407 (2018).
- [28] S. Mi, P. Burset, and C. Flindt, Electron waiting times in hybrid junctions with topological superconductors, *Sci. Rep.* **8**, 16828 (2018).
- [29] D. S. Kosov, Waiting time between charging and discharging processes in molecular junctions, *J. Chem. Phys.* **149**, 164105 (2018).
- [30] S. L. Rudge and D. S. Kosov, Distribution of waiting times between electron cotunneling events, *Phys. Rev. B* **98**, 245402 (2018).
- [31] S. L. Rudge and D. S. Kosov, Nonrenewal statistics in quantum transport from the perspective of first-passage and waiting time distributions, *Phys. Rev. B* **99**, 115426 (2019).
- [32] G. Engelhardt and J. Cao, Tuning the Aharonov-Bohm effect with dephasing in nonequilibrium transport, *Phys. Rev. B* **99**, 075436 (2019).
- [33] N. Ho and C. Emary, Counting statistics of dark-state transport through a carbon nanotube quantum dot, *Phys. Rev. B* **100**, 245414 (2019).
- [34] P. Burset, J. Kotilahti, M. Moskalets, and C. Flindt, Time-Domain Spectroscopy of Mesoscopic Conductors Using Voltage Pulses, *Adv. Quantum Technol.* **2**, 1900014 (2019).
- [35] S. L. Rudge and D. S. Kosov, Counting quantum jumps: A summary and comparison of fixed-time and fluctuating-time statistics in electron transport, *J. Chem. Phys.* **151**, 034107 (2019).
- [36] K. Wrzeniewski and I. Weymann, Current cross-correlations and waiting time distributions in Andreev transport through Cooper pair splitters based on triple quantum dots, *Phys. Rev. B* **101**, 155409 (2020).
- [37] L. S. Levitov, H. Lee, and G. B. Lesovik, Electron counting statistics and coherent states of electric current, *J. Math. Phys.* **37**, 4845 (1996).
- [38] D. A. Bagrets and Yu. V. Nazarov, Full counting statistics of charge transfer in Coulomb blockade systems, *Phys. Rev. B* **67**, 085316 (2003).
- [39] M. L. Mehta, *Random Matrices* (Elsevier, Amsterdam, 2004).
- [40] S. K. Gorman, Y. He, M. G. House, J. G. Keizer, D. Keith, L. Fricke, S. J. Hile, M. A. Broome, and M. Y. Simmons, Tunneling Statistics for Analysis of Spin-Readout Fidelity, *Phys. Rev. Applied* **8**, 034019 (2017).
- [41] M. Jenei, E. Potanina, R. Zhao, K. Y. Tan, A. Rossi, T. Tantt, K. W. Chan, V. Sevriuk, M. Möttönen, and A. Dzurak, Waiting time distributions in a two-level fluctuator coupled to a superconducting charge detector, *Phys. Rev. Research* **1**, 033163 (2019).
- [42] S. Matsuo, K. Kuroyama, S. Yabunaka, S. R. Valentin, A. Ludwig, A. D. Wieck, and S. Tarucha, Full Counting Statistics of Spin-Flip/Conserving Charge Transitions in Pauli-Spin Blockade, arXiv:1909.12027.
- [43] A. Kurzman, P. Stegmann, J. Kerski, R. Schott, A. Ludwig, A. D. Wieck, J. König, A. Lorke, and M. Geller, Optical Detection of Single-Electron Tunneling into a Semiconductor Quantum Dot, *Phys. Rev. Lett.* **122**, 247403 (2019).
- [44] J. König, H. Schoeller, and G. Schön, Zero-bias anomalies and boson-assisted tunneling through quantum dots, *Phys. Rev. Lett.* **76**, 1715 (1996).
- [45] C. Timm, Tunneling through molecules and quantum dots: Master-equation approaches, *Phys. Rev. B* **77**,

- 195416 (2008).
- [46] S. Koller, M. Grifoni, M. Leijnse, and M. R. Wegewijs, Density-operator approaches to transport through interacting quantum dots: Simplifications in fourth-order perturbation theory, *Phys. Rev. B* **82**, 235307 (2010).
- [47] K. Kaasbjerg and W. Belzig, Full counting statistics and shot noise of cotunneling in quantum dots and single-molecule transistors, *Phys. Rev. B* **91**, 235413 (2015).
- [48] A. Braggio, J. König, and R. Fazio, Full Counting Statistics in Strongly Interacting Systems: Non-Markovian Effects, *Phys. Rev. Lett.* **96**, 026805 (2006).
- [49] C. Flindt, T. Novotný, A. Braggio, M. Sasseti, and A.-P. Jauho, Counting Statistics of Non-Markovian Quantum Stochastic Processes, *Phys. Rev. Lett.* **100**, 150601 (2008).
- [50] C. Flindt, T. Novotný, A. Braggio, and A.-P. Jauho, Counting statistics of transport through Coulomb blockade nanostructures: High-order cumulants and non-Markovian effects, *Phys. Rev. B* **82**, 155407 (2010).
- [51] R. Zwanzig, *Nonequilibrium Statistical Mechanics* (Oxford University Press, Oxford, 2001).
- [52] D. Marcos, C. Emary, T. Brandes, and R. Aguado, Non-markovian effects in the quantum noise of interacting nanostructures, *Phys. Rev. B* **83**, 125426 (2011).
- [53] C. Emary and R. Aguado, Quantum versus classical counting in non-Markovian master equations, *Phys. Rev. B* **84**, 085425 (2011).
- [54] To evaluate the kernel $\mathbb{W}(s)$, we then multiply each diagram by the factor $s^{\max(n/2, 0)}$, where n is the number of counted black vertices.
- [55] A. Komnik and A. O. Gogolin, Full Counting Statistics for the Kondo Dot, *Phys. Rev. Lett.* **94**, 216601 (2005).
- [56] T. L. Schmidt, A. O. Gogolin, and A. Komnik, Full counting statistics of spin transfer through a Kondo dot, *Phys. Rev. B* **75**, 235105 (2007).
- [57] A. Komnik and H. Saleur, Full Counting Statistics of Chiral Luttinger Liquids with Impurities, *Phys. Rev. Lett.* **96**, 216406 (2006).
- [58] D. B. Gutman, Y. Gefen, and A. D. Mirlin, Full Counting Statistics of a Luttinger Liquid Conductor, *Phys. Rev. Lett.* **105**, 256802 (2010).